Journal of Chromatography, 192 (1980) 259–274
© Elsevier Scientific Publishing Company, Amsterdam — Printed in The Netherlands

CHROM. 12,623

FRACTIONATION OF POLYMERS BY GEL PERMEATION CHROMATOGRAPHY: AN EXPERIMENTAL AND THEORETICAL APPROACH

ARNO MAX BASEDOW, KLAUS HEINRICH EBERT*, HANNS JOSEF EDERER and ERICH FOSSHAG**

Institut für Angewandte Physikalische Chemie und SBF 123, Universität Heidelberg, D-6900 Heidelberg (G.F.R.)

(First received July 31st, 1979; revised manuscript received December 19th, 1979)

SUMMARY

The mechanism of gel permeation chromatography has been studied in a series of experiments performed on separation matrices of controlled pore glass with known pore structure and narrow pore size distribution, and using dextran fractions with accurately determined molecular weights and very narrow molecular weight distribution. Molecular weight calibration of the columns and effects of experimental variables on the shape of the elution peak and the peak broadening function were investigated, and the distribution and transport of polymer molecules between the mobile phase and the stationary phase within the pores of the separation material were discussed. An improved stochastic model for molecular weight calibration of separation matrices with cylindrical pores is developed as a function of the pore diameter.

INTRODUCTION

Although significant progress has been made in the understanding of the mechanism of gel permeation chromatography (GPC), a general and rigorous model has still not been achieved. Many systems have been studied and empirical relationships have been obtained for the dependence of the elution coefficient on the molecular weights (MW) of the polymers investigated. Most theoretical work, however, has been limited to very simplified pore network geometries and to idealized polymer molecule structures[1,2]. Though non-equilibrium is more likely to occur in GPC than in any other form of chromatography, because of the small diffusion coefficients of polymer molecules, it is now generally agreed that separation by GPC is governed by some kind of equilibrium partition of the polymer between the macroscopic mobile phase and the microscopic phases entrapped in the pores of the packing material. Stochastic evaluations for the equilibrium distribution of the

* To whom correspondence should be addressed.

** Extracted from a thesis submitted to the University of Heidelberg in partial fulfillment of the requirements for the degree of Doctor of Natural Sciences.

polymer molecules in an inert porous medium constitute the basis of the most useful models of GPC[3–5]. Another major problem of GPC is the quantitative evaluation of the peak broadening function (PBF). Here the difficulties lie in solving the complex equations for the highly tortuous flow along the irregularly shaped channels between the particles of the packing material.

The mechanism of GPC is the subject of the present study. Both MW calibration and the effect of experimental variables on the shape of the elution peak were thoroughly investigated. An improved stochastic model based on numerous experimental results is developed. Controlled pore glass (CPG) was used because of its unsurpassed mechanical stability, chemical inertness and constancy of pore structure. In addition, the average pore diameter and the very narrow pore size distribution can be accurately measured by electron micrography and mercury intrusion analysis[6], making it thus ideally suited for mechanistic studies. Dextran was selected as a polymer because of its well known conformational and solution properties[7,8], and the availability of fractions with extremely narrow molecular weight distribution (MWD) and precisely known MWs.

MATERIALS AND METHODS

Dextrans

Dextran fractions with narrow MWDs were prepared from commercially available products by preparative GPC on Sephadex and Sepharose (Pharmacia, Uppsala, Sweden) as described previously[9]. Oligomers, isomaltose and isomaltotriose were prepared by acid hydrolysis of dextran, followed by preparative GPC on Sephadex. The MWs of the fractions were determined by sedimentation equilibrium, low-angle laser light scattering and end-group analysis[9,10]. The MWs are summarized in Table I; deviations in the MW averages are within $\pm$ 4% for $\bar{M}_n$ and $\pm$ 1.5% for $\bar{M}_w$. Polydispersity of the very narrow fractions ($\bar{M}_w/\bar{M}_n \leqslant 1.02$) was determined by combination of GPC and light scattering. Fractions 1–18 were used to calibrate GPC columns; corrections of polydispersity were applied according to a previous publication[10]. Fractions I–III were prepared in large scale and characterized by GPC; they were used for peak broadening studies and to investigate the effects of flow-rate on the separation parameters.

Controlled pore glass

Investigations were carried out on columns packed with CPG (Electro Nucleonics, Fairfield, N.J., U.S.A.). All glasses were in the form of irregular particles in the range 100–250 μm. The particle size distribution was narrowed by sieving the commercial product; it was determined by microscopy that 95% of the material was within $\pm$ 10% of the nominal particle diameter. Average pore size and pore diameter distribution were determined by mercury intrusion analysis; 95% of the pore space was found to lie within $\pm$ 5% of the average pore diameter. For studies of peak broadening within the interstitial space of the column, a packing of non-porous glass was used. The characteristic data of the column packings are listed in Table II.

Equipment

Chromatographic runs were performed using essentially the same equipment

TABLE I

MOLECULAR WEIGHT AVERAGES OF NARROW DEXTRAN FRACTIONS

Fraction No.	$\overline{M}_n$	$\overline{M}_w$	$\overline{M}_w/\overline{M}_n$
1	685,000	735,000	1.07
2	438,000	440,000	1.01
3	286,000	288,000	1.01
4	145,000	163,000	1.12
5	73,200	74,000	1.01
6	51,000	54,100	1.06
7	29,900	30,200	1.01
8	22,100	22,400	1.01
9	16,000	16,800	1.05
10	12,400	13,100	1.06
11	8150	8540	1.05
12	5400	5700	1.06
13	3050	3330	1.09
14	2400	2650	1.10
15	990	1000	1.01
16	504	—	—
17	342	—	—
18	180	—	—
I	138,000	145,000	1.05
II	86,800	90,300	1.04
III	10,400	11,000	1.06

TABLE II

CHARACTERISTIC DATA OF CPG

Average pore diameter (nm)	*Average particle size (μm)*	*Average pore volume (ml g^{-1})*
34.4	102	1.16
34.7	152	1.17
65.4	241	1.05
Non-porous	196	—

described in a previous publication[11]. Comparatively short glass columns (250 × 11 mm I.D.) were used in order to allow very high flow-rates. A standard valve equipped with a loop was used to inject the polymer samples (2 mg dissolved in 0.5 ml). The eluent for all chromatographic investigations was water containing 0.2% potassium nitrate, added to prevent ghost peaks. Frontal experiments were performed with 0.03% dextran solutions and the same eluent.

Procedure

The exclusion volume, V_0, of the columns was determined with a high MW dextran ($\overline{M}_w = 5.2 \cdot 10^6$), and the total free volume, V_t, was measured with deuterium oxide at flow-rates ($\approx$ 20 ml cm^{-2} h^{-1}) where no dependence of the elution volume on the flow-rate could be detected and the peak shape was perfectly gaussian. The

elution volumes, V_e, of all dextran samples were taken at the maximum of the gaussian shaped peaks. For calibration purposes the elution coefficient, K

$$K = \frac{V_e - V_0}{V_t - V_0} \tag{1}$$

was used. It should be noted that the internal pore volume, V_i, obtained by mercury intrusion porosimetry is identical with the difference between V_t and V_0 determined chromatographically ($V_i = V_t - V_0$). This confirms that no adsorption effects occur during chromatography of dextran on CPG.

The elution diagram of an almost monodisperse polymer fraction ($\overline{M}_w/\overline{M}_n \approx 1.01$) corresponds to the PBF, which is characterized by the standard deviation σ. In this study narrow dextran fractions (Table I, fractions I–III) having lognormal MWDs were used for most experiments, and a gaussian-type correction was applied to compensate for the residual polydispersity[10]. At high flow-rates the PBF was found to become asymmetrical, so that the elution volume V_m, taken at the maximum of the curve, was different from the elution volume $V_{1/2}$, taken at the bisectrix of the peak area. For small asymmetries the leading branch of the peak was characterized by the standard deviation σ_l and the trailing branch by the standard deviation σ_t. The asymmetry A_s of the PBF is then defined as

$$A_s = \frac{\sigma_l}{\sigma_t} \tag{2}$$

An analogous analysis of the elution profile can be applied to frontal experiments. In Fig. 1 the elution profile of a typical frontal run is represented by curve F. Curve D is the differential form of curve F, from which it is easy to determine the values of σ_l and σ_t at the inflection points (or $2\sigma_l$ and $2\sigma_t$ at the intercepts of the tangents with the abscissa). The elution diagram of a polymer sample in ordinary chromatography is similar to curve D; the only difference is that the ordinate represents the concentration c (Fig. 1). For gaussian PBFs A_s is unity.

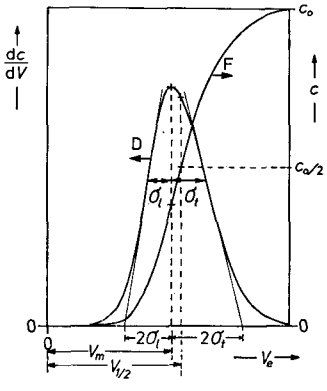

Fig. 1. Asymmetrical elution profile (concentration c *versus* elution volume V_e) of a frontal experiment (curve F) and its differential form (curve D). c_0, Final concentration of polymer; V_m, elution volume at maximum of curve D (or at inflection point of curve F); $V_{1/2}$, elution volume at bisectrix of peak area of curve D (or at $c_0/2$ on curve F); σ_l,σ_t, standard deviation of leading and trailing branch of curve D.

RESULTS

Calibration

The columns were calibrated under conditions where the elution volume of the MW standards was independent of the flow-rate and the elution peaks were of gaussian shape ($\dot{V} \approx 20$ ml cm^{-2} h^{-1}). A typical set of calibration curves of different types of CPG is shown in Fig. 2. High MW substances with elution volumes close to V_0 ($K < 0.15$) frequently had slightly asymmetric peaks. If the elution volume is taken at the maximum (V_m) of the chromatogram, short "upturns" occur in the calibration curves[11]. These "upturns" are more pronounced for broad pore size distributions and disappear if the elution volumes are taken at the bisectrix of the peak area ($V_{1/2}$). This procedure was generally adopted in this investigation.

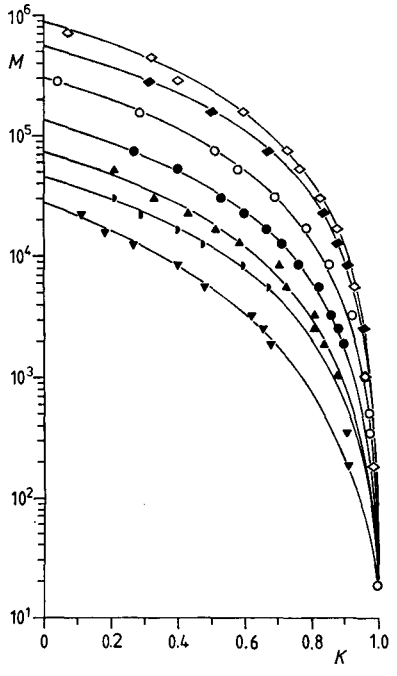

Fig. 2. Molecular weight (M) calibration curves for CPG; K is the elution coefficient (eqn. 1). Average pore diameters (nm): ◇, 65.4; ◆, 51.7*; ○, 34.7; ●, 22.7; ▲, 15.9*; ◗, 11.8*; ▼, 8.4*. (*, Data from ref. 11.)

As found empirically by Haller[12], a plot of log $(1-K)$ *versus* log M is linear (Fig. 3). The MW values extrapolated to $K = 0$ represent the critical MW (M_0) of dextran having the same dimensions as the pore size of the considered separation matrix of CPG[12]. Thus the calibration curves (Fig. 2) can be represented by the following equation

$$(1 - K) = \frac{M^a - M_t^a}{M_0^a - M_t^a} \tag{3}$$

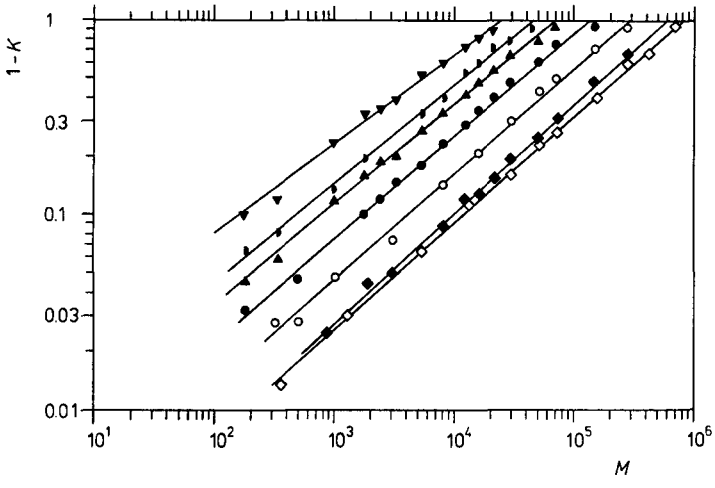

Fig. 3. Linearized calibration curves of Fig. 2.

where M_t is the limiting MW at $K = 1$ and a represents the slope of the straight lines in the polymer region in Fig. 3, and, as will be shown later, is a universal exponent. The values of M_0 and a were evaluated for $M_t = 20$ (deuterium oxide) using eqn. 3 and a least squares fit of the experimental points. The lines in Fig. 2 are the calculated calibration curves; in the low MW region several experimental points have been omitted for clarity. Table III lists the values of M_0 and a for CPG columns with different pore sizes. In Fig. 4 M_0 is plotted against the pore diameter d of the particular CPG in a double logarithmic scale. A straight line is obtained, from which eqn. 4 can be derived.

$$d = 0.0231 \cdot M^{0.581} \tag{4}$$

As it was assumed that the pore diameter of the packing material is equal to the dimension of the polymer molecule with MW M_0, d represents the equivalent sphere

TABLE III

CALCULATED VALUES OF THE CRITICAL MOLECULAR WEIGHT M_0 AND THE EXPONENT a (EQN. 4) FOR CPG WITH DIFFERENT PORE DIAMETERS

Average pore diameter (nm)	M_0	a
65.4	882,000	0.519
51.7	546,000	0.574
34.7	305,000	0.512
31.4	282,000	0.539
22.7	133,000	0.518
15.9	75,500	0.487
11.8	45,500	0.503
8.4	27,800	0.396

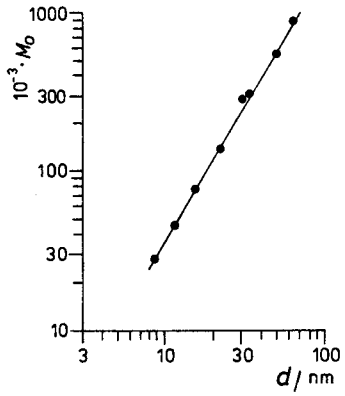

Fig. 4. Critical molecular weight (M_0) of dextran as function of the pore diameter (d) of CPG.

diameter of the respective molecule, and eqn. 4 is valid for every MW. The values of d obtained for given MWs are found to agree to within $\pm$ 20% with the equivalent sphere diameters obtained from diffusion, sedimentation and viscosity data. The exponent of 0.581 in eqn. 4 indicates that dilute salt solutions are good solvents for dextran.

Peak broadening

Investigations of peak broadening were carried out in three steps: instrumental broadening (σ_i), broadening within the void volume of the column (σ_v), and the combined broadening within the void and the pore volume of the column (σ_c). The instrumental PBF (sample of 0.5 ml plus valves and tubing of the chromatographic system) was found to be always asymmetrical but small compared with the broadening function of the column ($A_s = 0.7$, $\sigma_i = 0.25$ ml). Even though σ_t was not gaussian, the total broadening function (σ_t) was calculated from σ_i and σ_c according to eqn. 5.

$$\sigma_t = \sigma_i^2 + \sigma_c^2 \tag{5}$$

since σ_c was gaussian in most cases and always large compared with σ_i.

Fig. 5 shows σ_v for different MWs. The corresponding chromatograms were slightly asymmetrical ($A_s = 0.8$–0.9), probably because of some channeling due to the irregular shape of the particles of CPG. A direct relationship between σ_v and the diffusion coefficients of dextran can be seen in Fig. 5. Fig. 6 shows σ_c for different columns. The influence of the MW of the polymer is comparatively small. Almost perfect gaussian PBFs were obtained for all MWs at flow-rates less than 30 ml $cm^{-2}\,h^{-1}$. In Fig. 6 peak broadening is smallest for high MWs (for $K \approx 0$ the values are comparable with σ_v), then passes through a broad maximum in the range of optimum separation of the column, and finally decreases again for substances with $K \approx 1$. The appearance of this maximum and the fact that peak broadening is more pronounced in larger pores will be discussed later.

Dependence of separation parameters on flow-rate

The elution volume of dextran and glucose on CPG depends very little on the flow-rate $\dot{V}$ of the eluent. If the elution volume is taken at the maximum of the

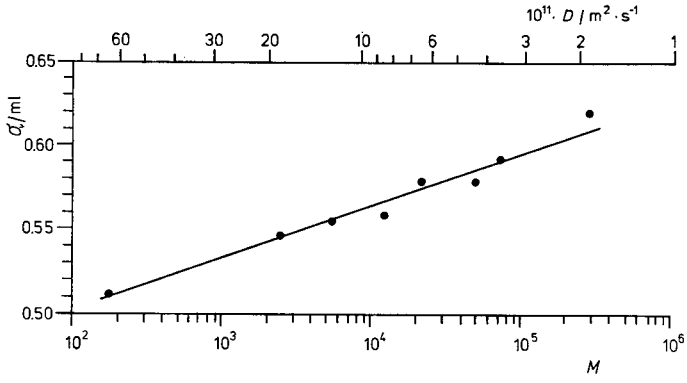

Fig. 5. Peak broadening function (σ_v) as function of the molecular weight (M) and diffusion coefficient (D) of dextran on non-porous glass; particle size, 196 μm; flow-rate, 20 ml cm^{-2} h^{-1}.

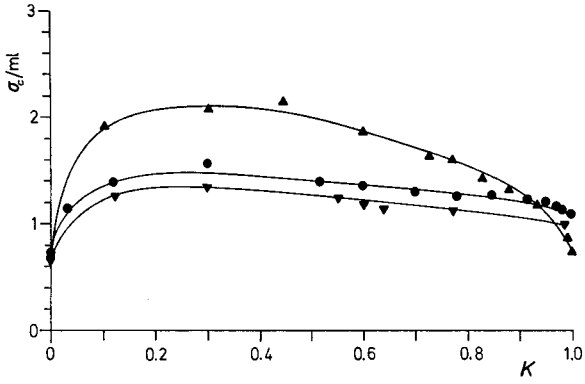

Fig. 6. Peak broadening function (σ_e) as function of the elution coefficient (K) of dextran on various columns of CPG at 20 ml cm^{-2} h^{-1}:

	Pore diameter (nm)	*Particle size (μm)*
▼	34.4	102
●	34.7	152
▲	65.4	241

peak, V_m, there is a small shift towards lower values for high $\dot{V}$, an effect which becomes more pronounced as the asymmetry of the peak increases. If the elution volume is, however, taken at the bisectrix of the peak area $V_{1/2}$, the shift with $\dot{V}$ is almost negligible (Fig. 7). Peak shift is of comparable magnitude on columns with different pore diameters, but decreases for smaller particle sizes of the packing material. Peak shift with flow-rate is thus caused mainly by asymmetrical peak broadening. In Fig. 7 solid lines were drawn if gaussian peaks were obtained, whereas dashed lines represent asymmetrical peaks. The effect of the flow-rate on the asymmetry is shown in Fig. 8.

On the other hand, the PBF depends strongly on $\dot{V}$. Although peaks are symmetrical for flow-rates of up to 40 ml cm^{-2} h^{-1}, σ increases markedly with $\dot{V}$,

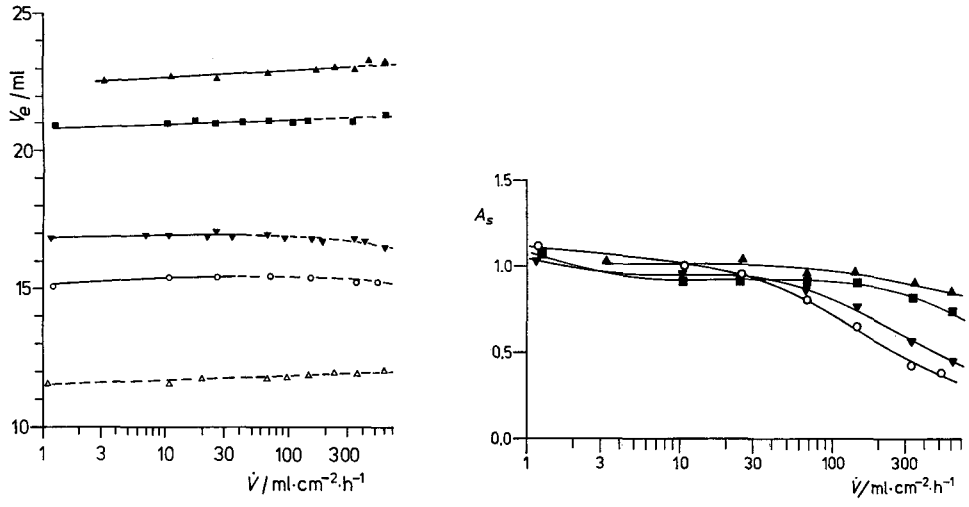

Fig. 7. Dependence of the elution volume (V_e) on the flow-rate ($\dot{V}$) on CPG (pore diameter, 34.7 nm; particle size, 152 μm). Solid lines refer to gaussian peaks ($V_e = V_{1/2} = V_m$); dashed lines refer to asymmetrical peaks ($V_e = V_{1/2} \neq V_m$). ▲, Glucose; ■, dextran ($\bar{M}_w$ 11,000); ▼, dextran ($\bar{M}_w$ 90,300); ○, dextran ($\bar{M}_w$ 145,000); △, dextran ($\bar{M}_w$ 5.2·10^6).

Fig. 8. Dependence of peak asymmetry (A_s) on the flow-rate ($\dot{V}$) for CPG (pore diameter, 34.7 nm; particle size, 152 μm). ▲, Glucose; ■, dextran ($\bar{M}_w$ 11,000); ▼, dextran ($\bar{M}_w$ 90,300); ○, dextran ($\bar{M}_w$ 145,000); △, dextran ($\bar{M}_w$ 5.2·10^6).

especially on CPG of large particle size. In Fig. 9 σ is represented as a function of the flow-rate for different dextran fractions; σ_v and σ_i are included. The comparatively large peak broadening on CPG is a result of the irregular shape of the particles and the relatively large particle size.

Peak asymmetry is also strongly dependent on $\dot{V}$ and increases for larger pore diameters and larger particle size of the packing material (Table IV). For flow-rates less than 30 ml cm^{-2} h^{-1}, peaks were of almost gaussian shape; for higher flow-rates peak asymmetry A_s was comparatively large. The effect is more pronounced for high MWs of the polymer investigated (Fig. 8). Asymmetry of peaks is caused mainly by the disturbed flow of the eluent within the interstitial volume around the irregularly shaped particles of CPG (curves B in Fig. 9). Therefore, column packing should be as perfect and dense as possible, because even small inhomogeneities strongly decrease peak symmetry.

Comparison between conventional chromatography and frontal experiments

In addition to the conventional elution experiments with injection of pulse samples, frontal experiments were carried out under the same conditions. Displacement of the eluent by polymer solutions, as well as displacement of polymer solutions by the eluent, was analysed in order to investigate the diffusion process of polymer molecules into and out of the matrix pores. No difference was found between the two procedures. Furthermore, as shown in Fig. 10, no difference in elution volume or peak shape was found between conventional pulse sample elution and frontal experiments, irrespective of flow-rate and MW of the polymer. This confirms that interactions

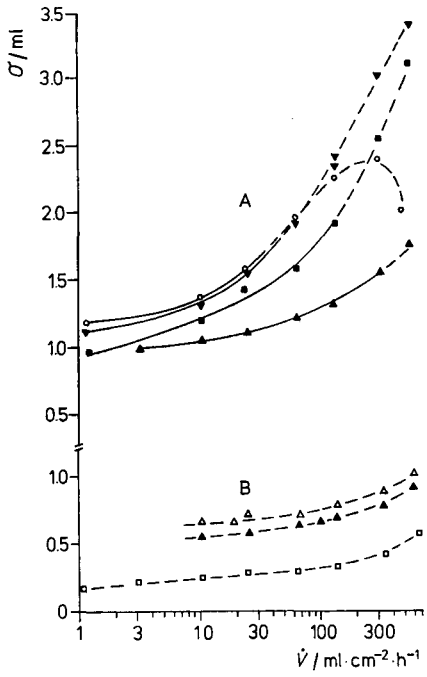

Fig. 9. Dependence of the peak broadening function (σ) on the flow-rate ($\dot{V}$) for CPG. Solid lines refer to gaussian peaks, dashed lines refer to asymmetrical peaks. Curves A: CPG (pore diameter, 34.7 nm; particle size, 152 μm); curves B: non-porous glass (particle size, 196 μm). ▲, Glucose; ■, dextran ($\bar{M}_w$ 11,000); ▼, dextran ($\bar{M}_w$ 90,300); ○, dextran ($\bar{M}_w$ 145,000); △, dextran ($\bar{M}_w$ $5.2 \cdot 10^6$); □, instrumental broadening function.

TABLE IV

EFFECT OF VARIATIONS IN PORE DIAMETER AND PARTICLE SIZE ON THE STANDARD DEVIATION (σ) AND THE ASYMMETRY (A_s) OF THE PBF

Flow-rate, 20 ml cm^{-2} h^{-1}; dextran $\bar{M}_w$, 145,000)

Average pore diameter (nm)	*Average particle size (μm)*	*σ (ml)*	A_s
34.4	102	1.37	0.98
34.7	152	1.48	0.98
65.4	241	1.78	0.89
22.7 + 51.7*	152	1.61	0.93

* Mixture of equal parts.

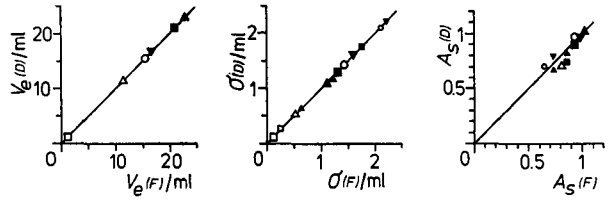

Fig. 10. Comparison between the elution volume (V_e), standard deviation (σ) and asymmetry (A_s) of the peak broadening function for conventional pulse injection chromatography (index D) and frontal experiments (index F) on CPG (pore diameter, 34.7 nm; particle size, 152 μm). ▲, Glucose; ■, dextran ($\bar{M}_w$ 11,000); ▼, dextran ($\bar{M}_w$ 90,300); ○, dextran ($\bar{M}_w$ 145,000); △, dextran ($\bar{M}_w$ $5.2 \cdot 10^6$); □, instrumental broadening function. Large symbols refer to a flow-rate of 20 ml cm^{-2} h^{-1}; small symbols to 100 ml cm^{-2} h^{-1}.

between polymer molecules and with the packing material of the column are negligible and insignificant in the mechanism of separation by GPC.

Additional effects

Separation experiments were also carried out on columns packed with non-porous glass. Small fractionation effects were found: dextrans with MWs of $150 \cdot 10^6$, $5.2 \cdot 10^6$, 145,000 and glucose were eluated after 11.23 ml, 11.45 ml, 11.51 ml and 11.58 ml, respectively. A similar effect on columns filled with non-porous glass beads was found by Pedersen[13]. This separation by size seems to be caused by the enhanced movement of the larger molecules relative to the smaller ones in the narrow channels between the particles of the packing material during elution[14]. The effect is, however, too small to play a noticeable role in GPC on porous media.

To gain further insight into the mechanism of GPC, partition coefficients were measured at static conditions. For this purpose, a measured amount of CPG was added to solutions of different dextran fractions or glucose of measured concentration, and the concentration outside the porous glass after equilibrium was determined refractometrically[15,16]. It was found that the values obtained for these static partition coefficients were in agreement to within $\pm$ 20% with the values determined by conventional elution chromatography (Table V). These results explain the small effect that the flow-rate has on the elution volume in conventional chromatography (Fig. 7). Furthermore, the agreement between the partition coefficients determined by both methods indicates that GPC is an equilibrium process of separation.

TABLE V

COMPARISON BETWEEN THE PARTITION COEFFICIENTS OF STATIC MEASUREMENTS (K_s) AND CONVENTIONAL ELUTION CHROMATOGRAPHY (K)

Average pore diameter (nm)	*Substance*	*Molecular weight,* $\overline{M}_w$	K_s	K
312	glucose	180	0.91	1.00
65.4	glucose	180	0.90	1.00
34.7	potassium nitrate	101	0.97	1.00
34.7	dextran	11,000	0.79	0.82
34.7	dextran	88,500	0.44	0.47
34.7	dextran	116,000	0.39	0.39
34.7	dextran	$5.2 \cdot 10^6$	0.17	0.00

Investigations on the effect of viscosity on the separation parameters were carried out by adding high concentrations of sucrose ($\approx 257\ g\ l^{-1}$) to the eluent. The relative increase in viscosity compared with the standard eluent was 2.25. No influence on V_e or A_s was observed, but σ was increased by 15%. The most interesting phenomenon observed during chromatography in highly viscous media is a "storage effect", which is found when the flow-rate of the eluent is suddenly changed. If the flow-rate is increased, the concentration jumps immediately and remains almost constant until a volume equal to the liquid volume of the column ($\approx V_0$ for non-porous and $\approx V_t$ for porous glass) has passed through the column. A similar, but

less pronounced effect is observed if the viscosity of the eluent is increased by the same factor by the addition of dextran ($\approx 44\ g\ l^{-1}$; $\bar{M}_w = 38{,}000$). Fig. 11 shows the effect for porous and non-porous glass. Conversely, a decrease in concentration is found if the flow-rate is suddenly reduced. This effect can be explained by assuming that a boundary layer of solute (sucrose or dextran) is formed on the surface of the packing material accessible to the eluent, the thickness of which changes with flow-rate. This boundary layer seems to be formed by preferential adsorption of the solute on CPG. At low concentrations of solute, water is adsorbed on CPG, so that this effect is not observed under the usual conditions of chromatography.

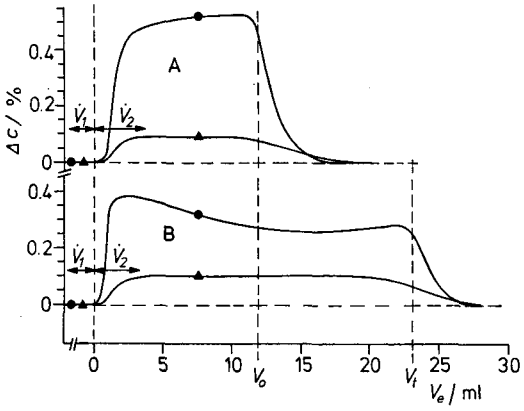

Fig. 11. Concentration jump ($\triangle c$ *versus* elution volume V_e) for a sudden increase of flow-rate from $\dot{V}_1 = 1$ ml cm^{-2} h^{-1} to 25 ml cm^{-2} h^{-1} during chromatography. Relative viscosity of eluents, 2.25 (●, sucrose; ▲, dextran $\bar{M}_w$ 38,000). Curves A: non-porous glass (particle size, 196 μm); curves B: CPG (pore diameter, 34.7 nm; particle size, 152 μm).

DISCUSSION

The dependence of the separation parameters on flow-rate and packing characteristics of chromatographic columns has been studied by Ouano and Barker, who developed a phenomenological model for GPC, based on diffusion processes[17,18]. This model treats the chromatographic column as two continuous phases, a mobile phase in which the molecules undergo molecular and eddy diffusion, and a stationary phase where the molecules undergo partition and molecular diffusion. For the simulation of the chromatographic process, material balances are established, boundary and initial conditions are fixed, and the set of partial differential equations obtained is solved by numerical methods. The model gives no information about the partition coefficient, K. It makes it possible, however, to predict the effect of experimental variables on the shape of the elution diagram of a given polymer sample. The following results were obtained from Ouano's simulations.

(1) The elution volume V_e, the standard deviation σ and the asymmetry A_s of the PBF depend on the flow-rate. The predicted dependences were found at least qualitatively in this study (Figs. 7–9).

(2) The σ-values of the PBF depend on the MW of the polymer; a maximum should exist for a certain MW. This is also verified by experiment (Fig. 6).

(3) The σ-values of the PBF increase for larger pore diameters and with increasing particle size. Experimental results which confirm this statement are shown in Fig. 6.

(4) The asymmetry A_s of the PBF increases for larger pore diameters and increasing particle size. This is in agreement with experiment (Table IV).

(5) Broad pore size distributions increase the σ-value of the PBF. The experimental results are also in agreement with this statement (Table IV).

In order to obtain the partition coefficient K from the MW of the polymer and the pore diameter of the packing material, a stochastic model of the separation process was developed in this study. It is assumed that as a polymer sample in dilute solution percolates through the column, the molecules will achieve a partition equilibrium with distribution coefficient K between the mobile phase and the stationary phase inside the pores of CPG. The polymer molecules are considered to be random coils, showing no adsorption on the separation matrix, and polymer–solvent interactions are not altered in the vicinity of the surface of the pores. These assumptions are supported by experiment, *e.g.* identical separation parameters for pulse sample elution and frontal experiments, and the same equilibrium distribution coefficients for elution chromatography and static experiments. As the polymer molecules are considered to be highly diluted, conformational changes are not accompanied by enthalpic effects. Therefore, it can be assumed that the free enthalpy changes during the transference of a polymer molecule from the mobile phase into a pore are caused exclusively by conformational entropy changes due to the limiting geometry of the pores. This loss in entropy, which is largest for a polymer molecule in the immediate vicinity of the walls of a pore, is assumed to be the ultimate cause of the partial exclusion of the polymer from the inside of the pores. The distribution coefficient K is defined as usual, *i.e.* the ratio of the concentration of polymer molecules within the porous medium to the concentration in the mobile phase.

The standard entropy of one mole of polymer within the pores, S_p^0, is proportional to the logarithm of the number, W_p, of geometrically allowed conformations within the pores:

$$S_p^0 = R \ln W_p \tag{6}$$

Similarly, the standard entropy, S_0^0, of the polymer outside the porous medium is:

$$S_0^0 = R \ln W_0 \tag{7}$$

where W_0 is the number of all possible conformations of the polymer. As $\Delta H^0 = 0$, the standard free enthalpy of transference, ΔG_0^0, of a mole of polymer from the mobile phase into the pores is:

$$\Delta G^0 = -T\Delta S^0 = -RT \ln K = -RT \ln \frac{W_p}{W_0} \tag{8}$$

The distribution coefficient $K = W_p/W_0$ is thus the ratio of the allowed conformations of the polymer molecule within the separation matrix to those in the

mobile phase. To determine K it is thus necessary to calculate the number of allowed conformations of a polymer molecule with a given MW within a certain pore and to relate this to the number of all possible conformations. Fig. 12 shows examples of a forbidden conformation (A) and an allowed conformation (B).

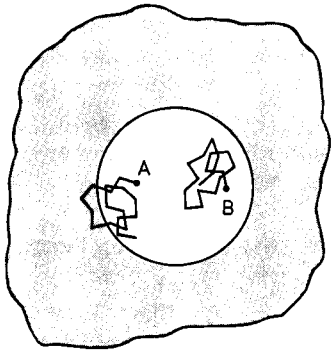

Fig. 12. Schematic representation of a random flight polymer chain within a cylindrical pore. A, forbidden conformation; B, allowed conformation.

Casassa[4,5] developed a similar stochastic model by solving the partial differential equations for the Brownian motion of a particle subjected to appropriate boundary conditions imposed by the walls of the pores. He derived a number of relationships between the partition coefficient and the dimensions of the macromolecules for pores of different geometry. A test of Casassa's equation for cylindrical pores gave good agreement with the present experiments in the high MW region, but large deviations occurred for low MWs. The reason for these deviations is that Casassa's approach is correct only if the number of segments of the polymer chain is large enough to balance out statistical fluctuations, *i.e.* for high MWs.

In the present study the numbers of allowed and forbidden conformations of a polymer with definite MW were calculated in cylindrical pores by means of a Monte Carlo method. Electron micrography[6] shows that CPG pores are approximately cylindrical. For the simulation the pore of radius r is defined by $r^2 \geqslant x^2 + y^2$; the length of the pore (z-axis) is not restricted. Every point within the pore has the same probability to be the starting point of a polymer molecule, *i.e.* two random numbers (x_0,y_0) were chosen for it, which obey the conditions $-r \leqslant x_0, y_0 \leqslant r$ and $x^2 + y^2 \leqslant r^2$. The polymer molecules are built up by adding three-dimensional random vectors with constant length l. The conditions $-1 \leqslant x,y,z \leqslant 1$ and $s = \sqrt{x^2 + y^2 + z^2} \leqslant 1$ are imposed, and the vectors are normalized to the length l of the statistical segment of the chain, *i.e.* for the i-th segment there is $x_1 = xl/s$, $y_1 = yl/s$ and $z_1 = zl/s$. This procedure was repeated until the molecule was completed. Only those molecules that can exist without steric restrictions within the pore are considered to have allowed conformations; from their number and the number of starting points for molecules the partition coefficient K was calculated. At least 2000 molecules were generated in this way for every MW. The universal calibration curve was constructed by repeating this procedure for *ca.* 50 different MWs (Fig. 13), from the monomer up to MWs of more than 10^6.

From the stochastic model of GPC it follows that a universal calibration curve should be obtained if the quantity $M \cdot r^{-2}$ is plotted against some function of K. As shown by Haller[12], the elution behaviour of polymer molecules is best charac-

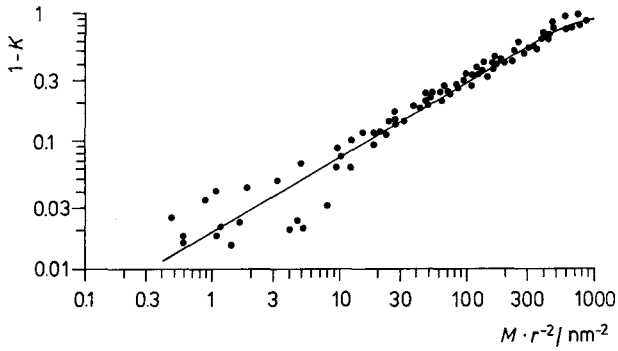

Fig. 13. Comparison of experimental values (●) of the elution coefficient (K) and the corresponding molecular weight (M) on columns of CPG with different pore radii (r) with the universal calibration curve (solid line), calculated by the Monte Carlo simulation of the stochastic model.

terized by the quantity $(1-K)$. In a double logarithmic scale a plot of $(1-K)$ *versus* Mr^{-2} is approximately linear; for a large number of experimental points obtained on CPG of different pore sizes this relationship is shown in Fig. 13. In the low MW region ($K > 0.9$) the experimental points are scattered, mostly owing to the double logarithmic scale. The Monte Carlo computations (curve in Fig. 13) were carried out in terms of the dimensionless group $Mlg/M_{mon}r^2 = Nl^2/r^2$, where l is the length of the statistical chain segment, N is the number of statistical chain segments of the molecule (contour length Nl), g is the length of the monomer unit (for glucose, $g = 0.515$ nm) and M_{mon} (= 162) is the MW of the monomer unit of dextran. During the computations the value of l was adjusted to obtain the best fit of the simulated calibration curve to the experimental points; variations in l cause a parallel shift of the calibration curve. The optimum value of l was found to be 0.525 nm, which is several times smaller than the experimental value of 2.04 nm obtained from low-angle X-ray scattering measurements[8]. One reason for this comparatively large discrepancy is that dextran molecules are branched, and not strictly linear as assumed in the Monte Carlo calculations. Deviations towards smaller values of l (by a factor of 1.5–2) cna be understood, as dextran molecules in solution are relatively compact coils[7], which is also confirmed by the unusually small radii of gyration[8] and molecular dimensions compared with the linear polymer. Furthermore, the equivalent sphere diameters obtained from GPC measurements (eqn. 4) are always smaller (by a factor of 1.2–1.5) than the dimensions of the molecules calculated from the corresponding radii of gyration, thus giving, at least qualitatively, an explanation for the low values of l obtained from the simulation. Current experiments with linear dextrans will give more detailed information about the discrepancy between theory and experiment. The stochastic model describes quantitatively the elution behaviour of dextran on columns of CPG with different pore diameters, if l is taken as a variable, thus enabling the calculation of calibration curves without further assumptions.

CONCLUSION

The experimental results and the theoretical approach presented in this paper show that the separation process in GPC can be explained by assuming equilibrium distribution between the mobile and the stationary phases within the porous matrix.

Therefore, it is relatively simple to compute the partition coefficients of polymer molecules of different MW in pores of constant radius by applying stochastic methods. The elution volume and the broadening function inherent to the separation process can then be calculated as functions of the MW and the pore dimensions. Additional broadening and the asymmetry of the elution peak, caused by transport processes, can be understood in terms of the model of Ouano, in which diffusion governs the establishment of the equilibrium distribution between the two phases.

The system used in the present investigation was well suited for basic mechanistic studies of GPC. The pores of CPG are nearly uniform and cylindrical, and dextran is a compact and stable polymer molecule with a coiled conformation in solution, which is available in fractions of very narrow MWD. The only remaining open question is the discrepancy between the values for the length of the statistical chain segment. The disagreement can be caused partly by enthalpy effects during conformational changes or by small alterations in the shape of the polymer molecules during migration into the pores of the separation matrix.

Finally, it should be mentioned that the experimental data of the present work fit straight lines for all pore sizes of CPG investigated, if log K is plotted against $M^{2/3}$. Such a dependence is characteristic for the partition equilibrium of the polymer between two phases, assuming that this process depends on the area of the polymer molecule[19]. This also results from our stochastic approach, as long as the conformation of dextran is coiled or spherical, and is identical within the mobile and the stationary phases. The log $K - M^{2/3}$ relationship is of central importance for the study of conformational changes of polymer molecules within the porous matrix during separation. Investigations of these effects are in progress.

ACKNOWLEDGEMENT

Financial support by the Deutsche Forschungsgemeinschaft and the Fonds der Chemischen Industrie is gratefully acknowledged.

REFERENCES

1 K. Altgelt and L. Segal, *Gel Permeation Chromatography*, Marcel Dekker, New York, 1971.
2 K. Altgelt, *Adv. Chromatogr.*, 7 (1968) 3.
3 J. Carmichael, *J. Polym. Sci., Part A-2*, (1968) 517.
4 E. Casassa, *J. Polym. Sci., Polym. Lett.*, 5 (1967) 773.
5 E. Casassa, *J. Phys. Chem.*, 75 (1971) 3929.
6 W. Haller, *Nature (London)*, 206 (1965) 693.
7 A. Basedow and K. H. Ebert, *J. Polym Sci., Polym. Symp.*, 66 (1979) 101.
8 S. Garg and S. Stivala, *J. Polym. Sci., Polym. Phys.*, 16 (1978) 1419.
9 A. Basedow, K. H. Ebert, H. Ederer and H. Hunger, *Makromol. Chem.*, 177 (1976) 1501.
10 A. Basedow, *Proceedings of the Second Deutsche Diskussionstagung für Anwendung der HPLC*, Waters Assoc., October 1977, Königstein/Taunus, pp. 175–200.
11 W. Haller, A. Basedow and B. König, *J. Chromatogr.* 132 (1977) 387.
12 W. Haller, *Macromolecules*, 10 (1977) 83.
13 K. Pedersen, *Arch. Biochem. Biophys.*, Suppl. 1 (1962) 157.
14 E. DiMarzio and C. Guttman, *J. Polym. Sci., Polym. Lett.*, 7 (1969) 267.
15 Z. Grubisic-Gallot and H. Benoit, *J. Chromatogr. Sci.*, 9 (1971) 262.
16 W. Yau, C. Malone and S. Fleming, *J. Polym. Sci., Polym. Lett.*, 6 (1968) 803.
17 A. Ouano and J. Barker, *Separ. Sci.*, 8 (1973) 673.
18 A. Ouano, *Adv. Chromatogr.*, 15 (1977) 233.
19 S. Hjertén, *J. Chromatogr.*, 50 (1970) 189.